Detector configuration

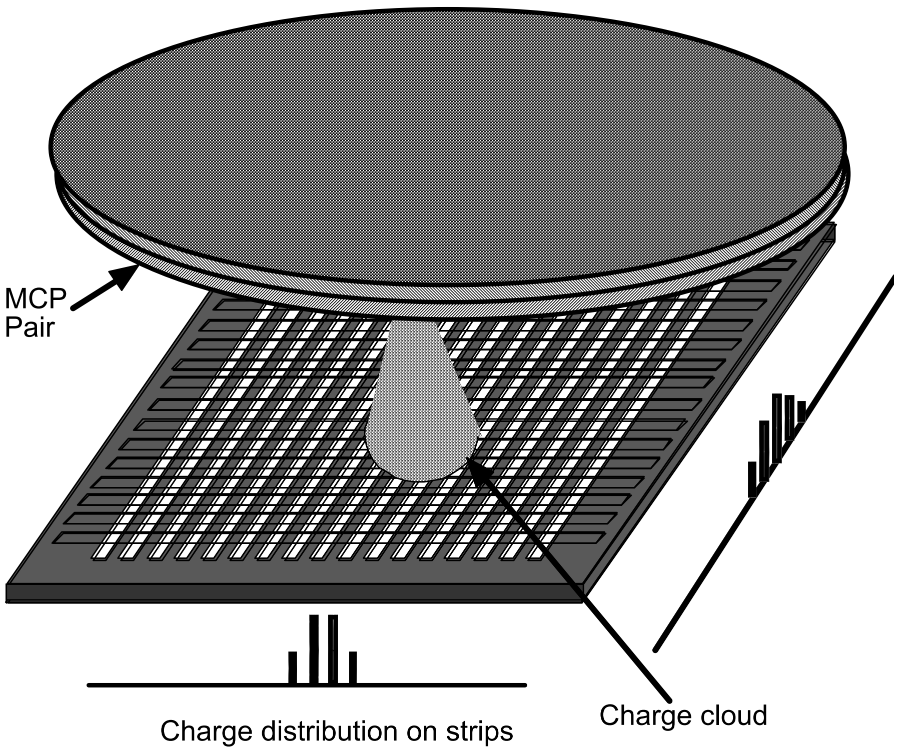

Schematic of an MCP detector

- Photon/ion/atom/neutron counting
- XY coordinates (<20 μm) and timing (<130 ps) information for each registered particle
- Selective detection of ions, electrons, photons
- Count rate ~MHz with 10% dead time
- No dark/readout noise!

Detector hardware implementations

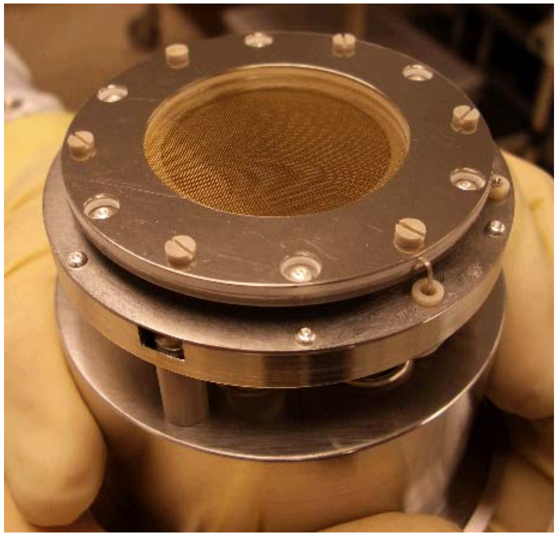

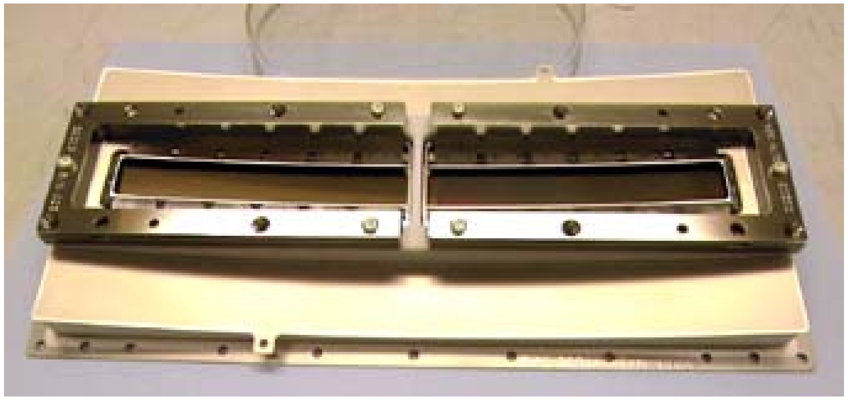

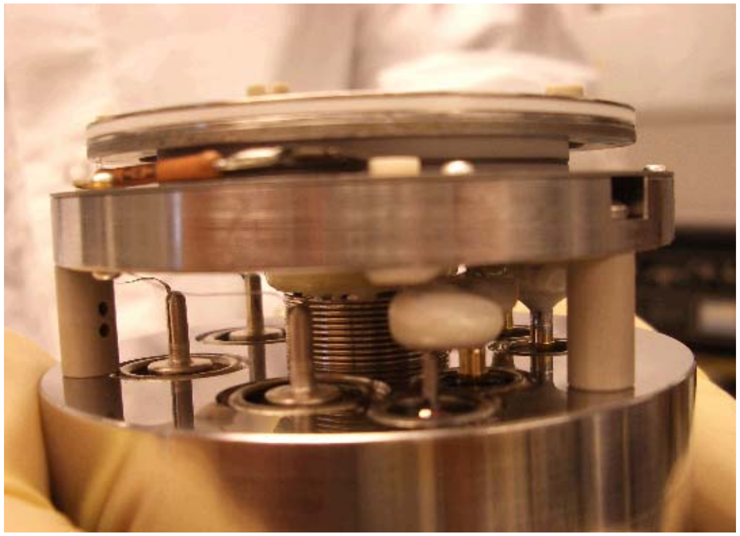

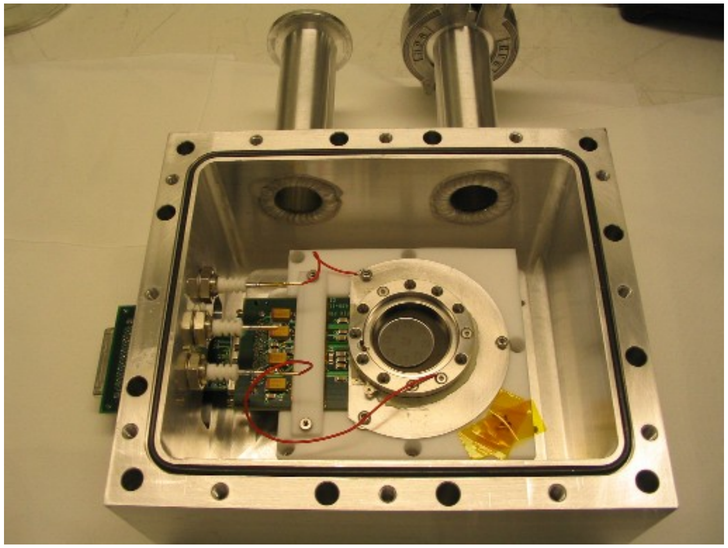

Experimental setup

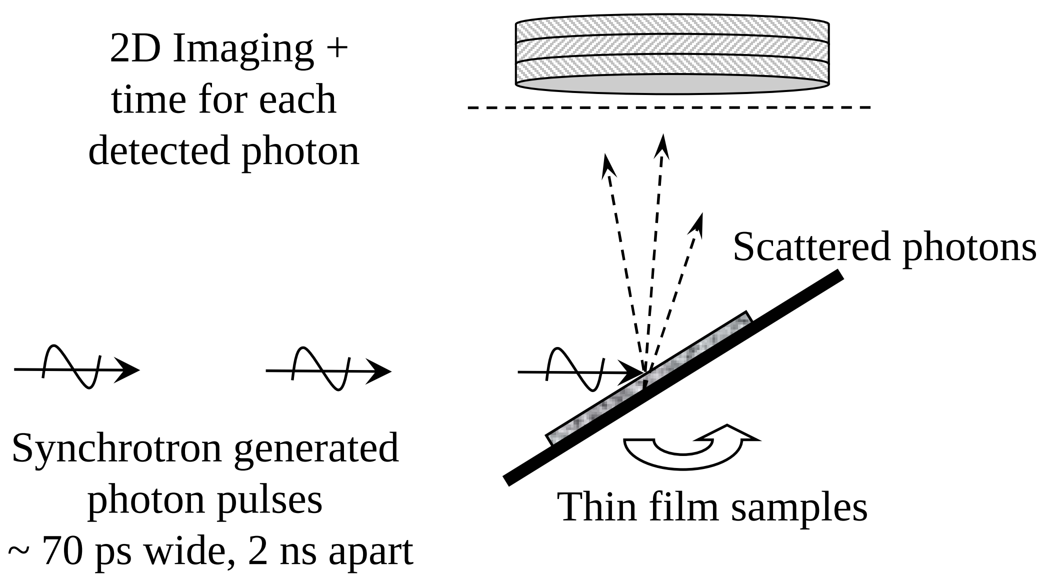

A. S. Tremsin, et al., IEEE Trans. Nucl .Sci. 54 (2007) 706.

A. S. Tremsin, et al., Nucl. Instr. Meth. A 580 (2007) 853.

Timing resolution

Elastically scattered photons

Timing accuracy 55 ps RMS (130 FWHM)

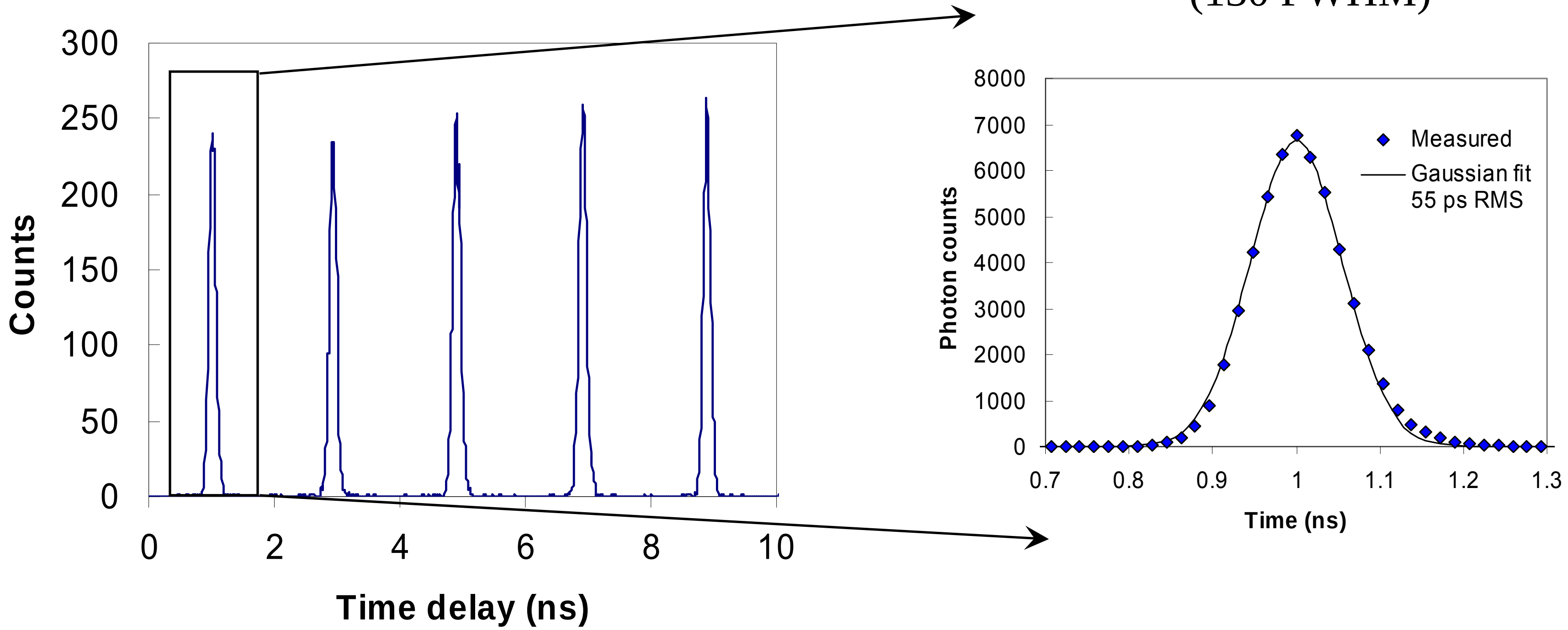

A. S. Tremsin, et al., IEEE Trans. Nucl .Sci. 54 (2007) 706.

A. S. Tremsin, et al., Nucl. Instr. Meth. A 580 (2007) 853.

Time histograms for different films

Only elastic scattering

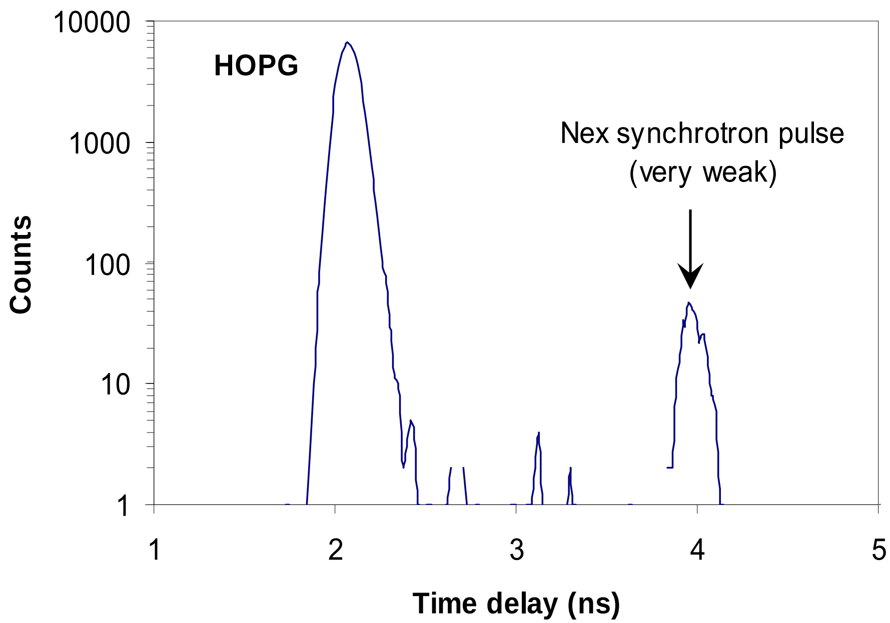

Both elastic and inelastic scattering are present

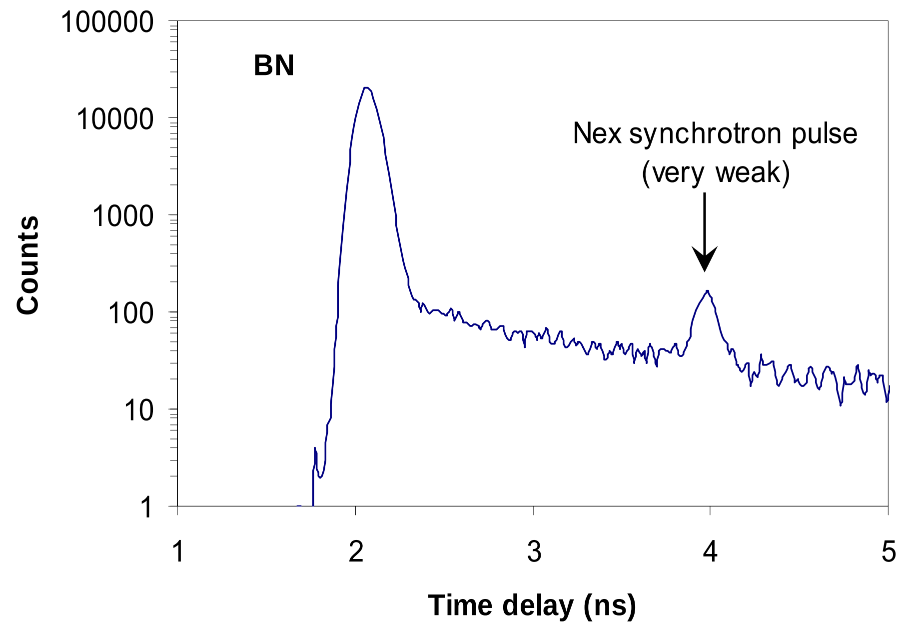

A. S. Tremsin, et al., IEEE Trans. Nucl .Sci. 54 (2007) 706.

Time histograms & images: photons vs. electrons

Photons detected,
electrons repelled by input mesh

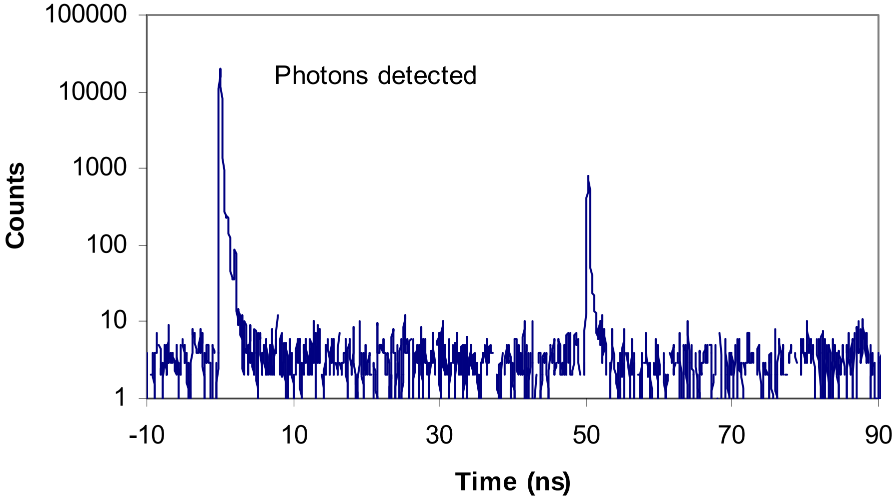

Time window selected for
only electron detection

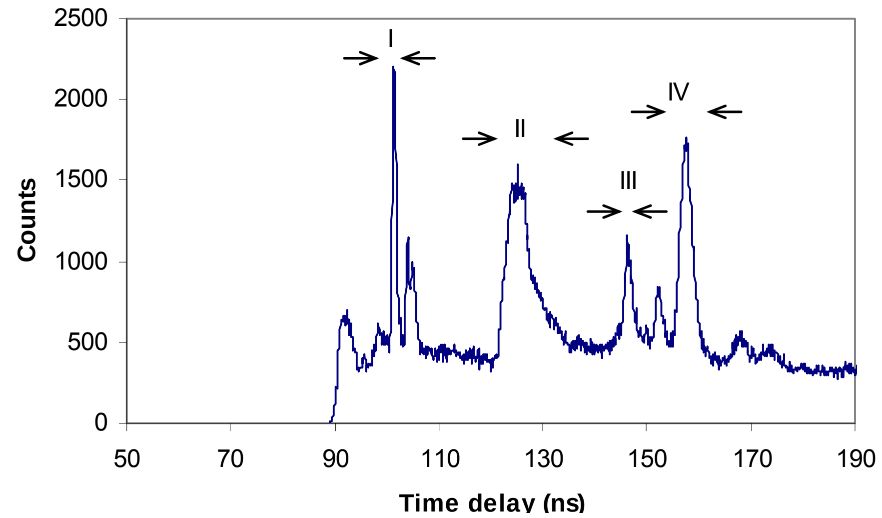

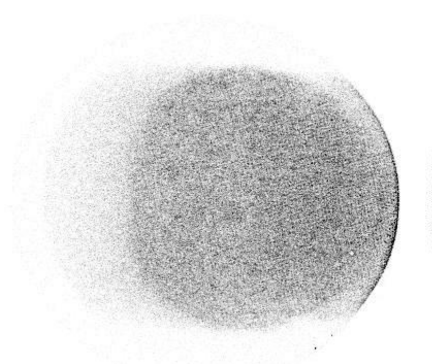

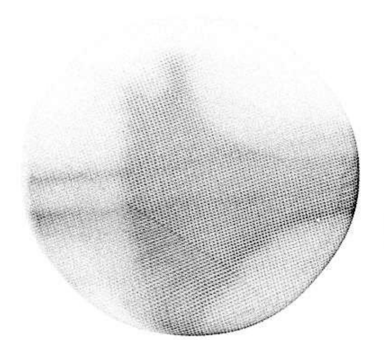

A. S. Tremsin, et al., Nucl. Instr. Meth. A 580 (2007) 853.

Images: electrons from different peaks

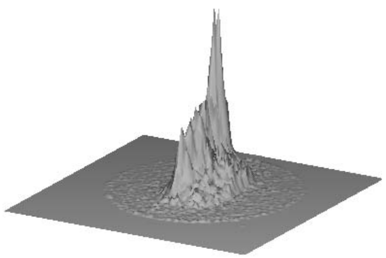

Only region I

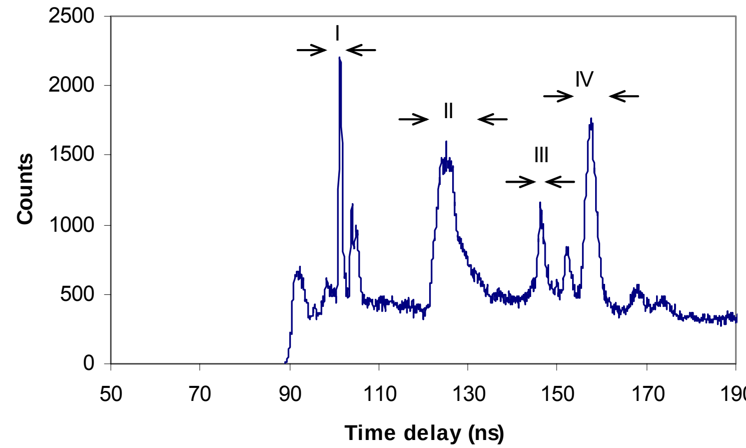

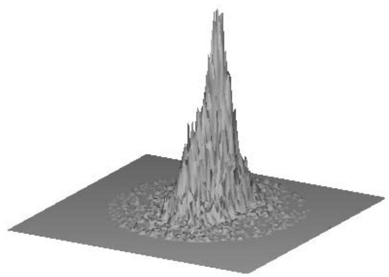

Only region II

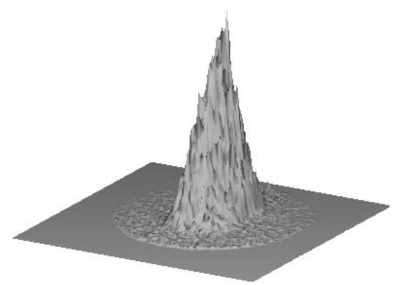

Only region III

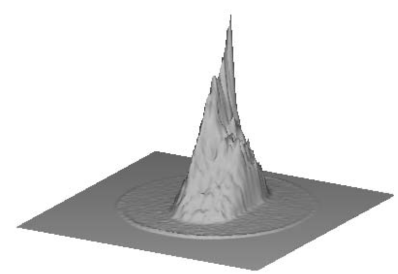

Entire histogram

A. S. Tremsin, et al., Nucl. Instr. Meth. A 580 (2007) 853.

Synchrotron bunch diffusion

Bunch population after injection

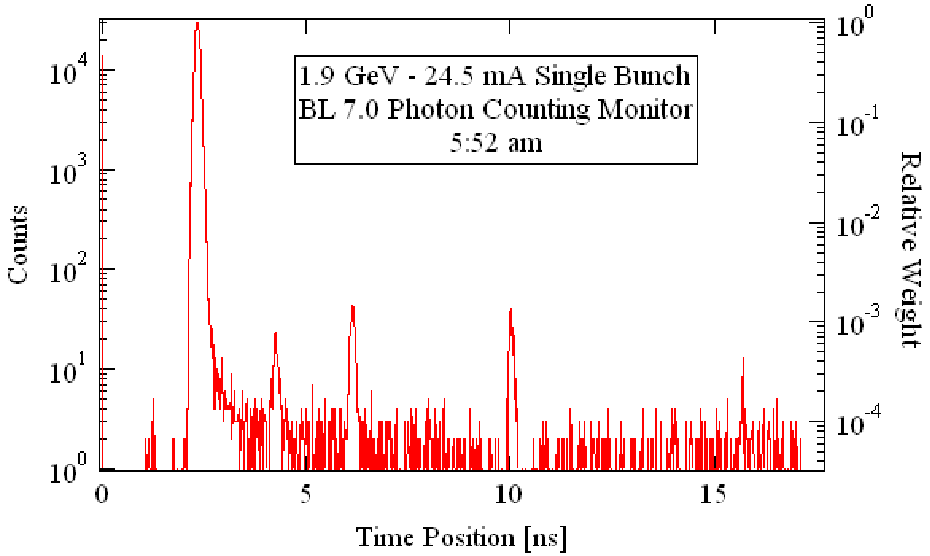

Bunch population ~76 min later

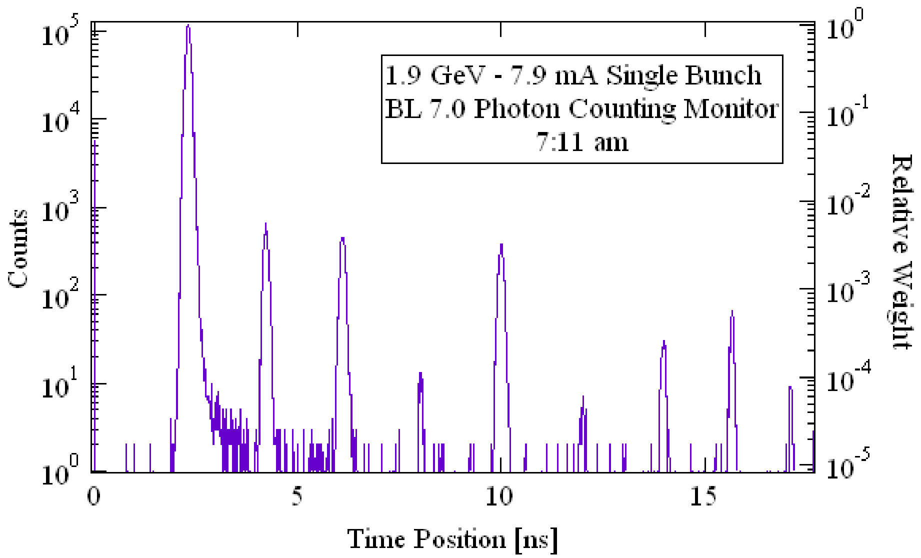

Diffusion of electrons between the adjacent bunches can be studied with the detection system

W. E. Byrne, C.-W. Chiu, J. Guo, F. Sannibale, J.S. Hull, O.H.W. Siegmund, A. S. Tremsin , J.V. Vallerga
Proceedings EPAC'06, Edinburgh, June 2006

Linearity of measured timing

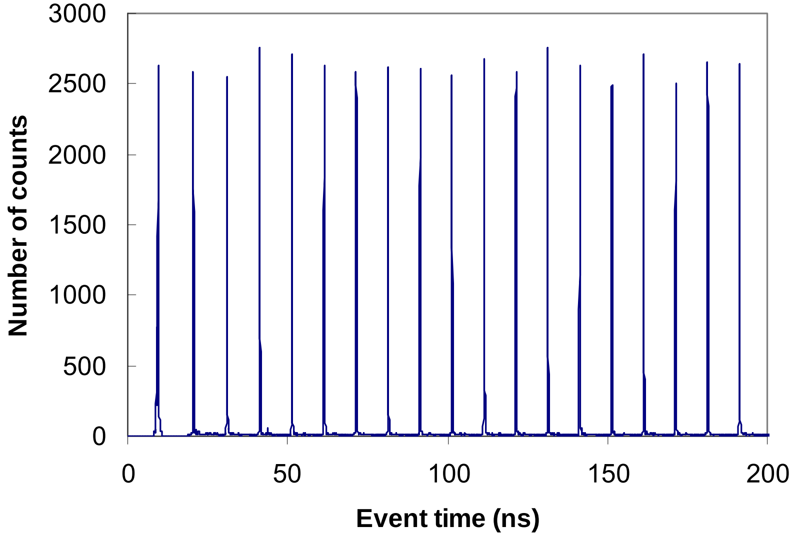

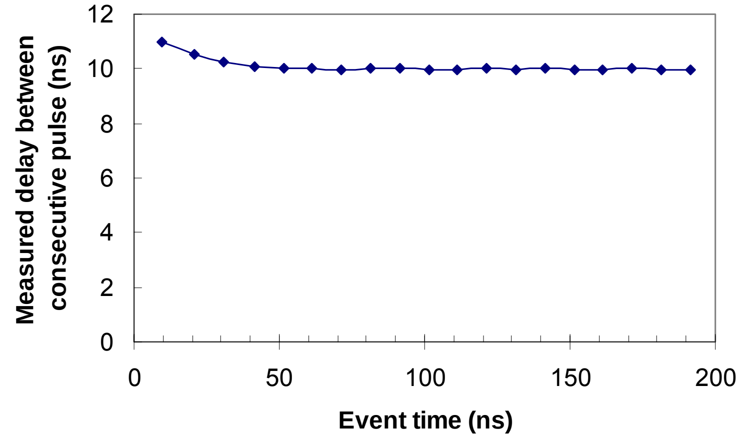

Measured timing histogram of electron pulses separated by 10 ns.

A. S. Tremsin, et al., Nucl. Instr. Meth. A 582 (2007) 168.

Spatial resolution: photons and electrons

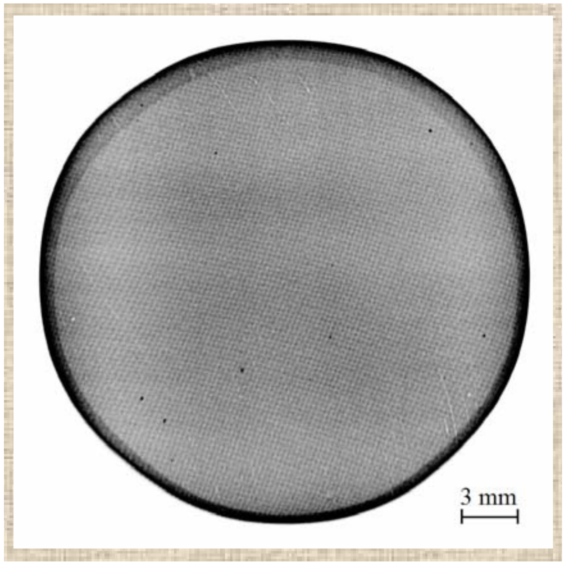

Phothon image
Full field illumination
25 mm active area
Mesh with 250 µm rectangular cells

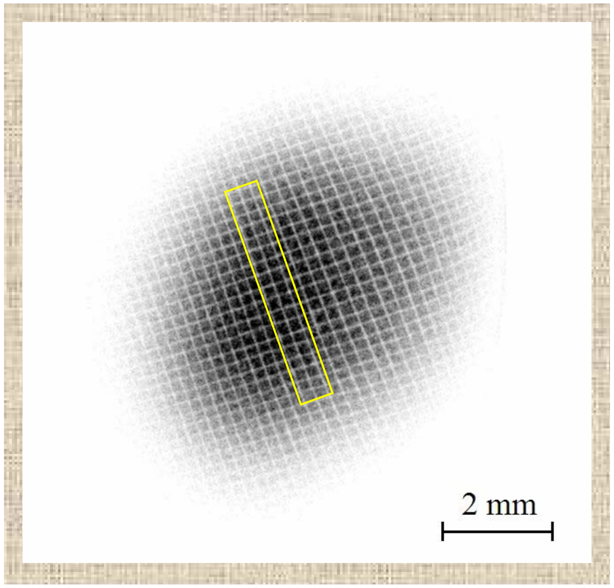

Electrons imaged
25 µm wires on 250 µm grid resolved

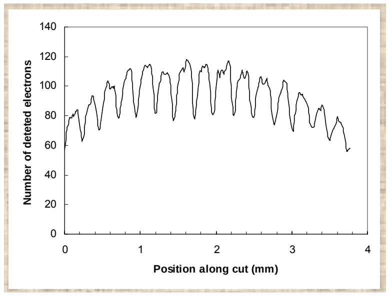

Cross section of electron image
25 µm wires are resolved

A. S. Tremsin, et al., Nucl. Instr. Meth. A 582 (2007) 168.

Spatial resolution of MCP detectors

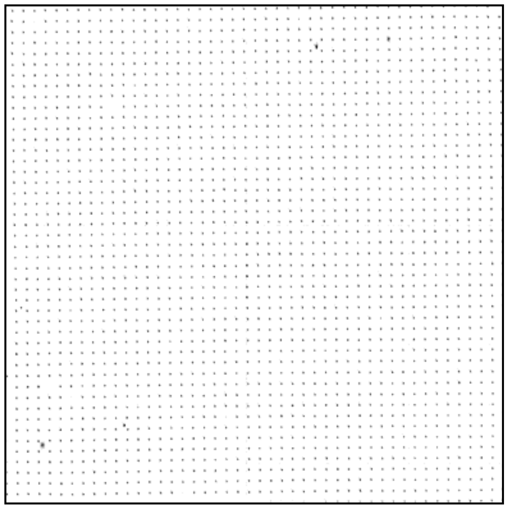

•**XDL readout**

•Very linear images

•Resolutions ~25µm FWHM

•Large Formats (10cm x 10cm)

•Event rates ~0.5 MHz

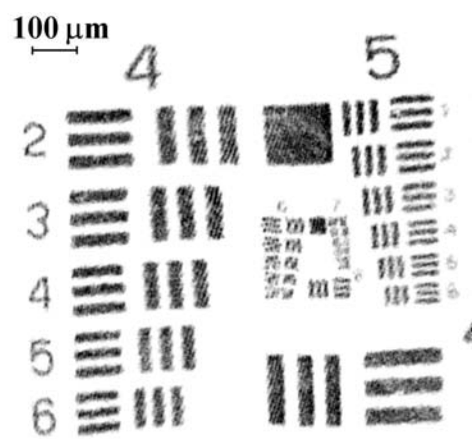

•**XS readout**

•Very high resolution

~12 µm FWHM @ <100 kHz

~20 µm FWHM @ few MHz

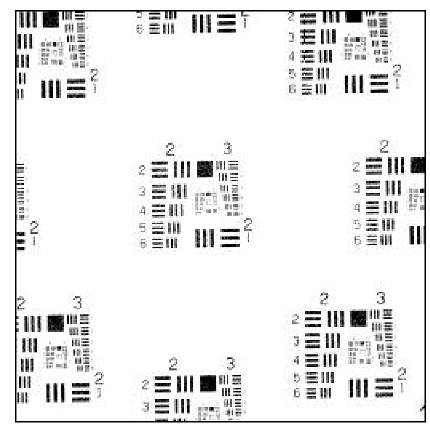

•**CMOS readout**

•Resolution ~55µm FWHM

•Very high event rates >1 GHz

MCP thermal runaway

$$R_{\mathrm{MCP}}(T_{\mathrm{MCP}}, V_{\mathrm{MCP}}) = R_0[1-\alpha_v V_{\mathrm{MCP}}]\exp\{-\beta_T(T_{\mathrm{MCP}}-T_0)\}, \quad (1)$$

α_T=0.015 C^{-1}

where R_0 is the resistance of MCP measured at $V_{\mathrm{MCP}}=0$ V and temperature $T_{\mathrm{MCP}}=T_0$.

Stable operation when $Q_{\mathrm{joule}}=Q_{\mathrm{rad}}+Q_{\mathrm{cond}}$.

$$Q_{Rad} = \frac{\pi \cdot D_0^2}{4} \cdot \sigma \cdot \epsilon \cdot (T_{MCP}^4 - T_A^4)$$

ϵ the effective thermal emittance (ϵ=0.4

heat dissipation from the MCP of only 0.015 $W \cdot cm^{-2}$ for T_{MCP}= 70 °C

A.S. Tremsin et al., Proc. SPIE **2808** (1996) pp.86-97.
A.S. Tremsin et al., Nucl. Instr.Meth. **379** (1996) pp.139-151.

Thermal Stability of MCPs

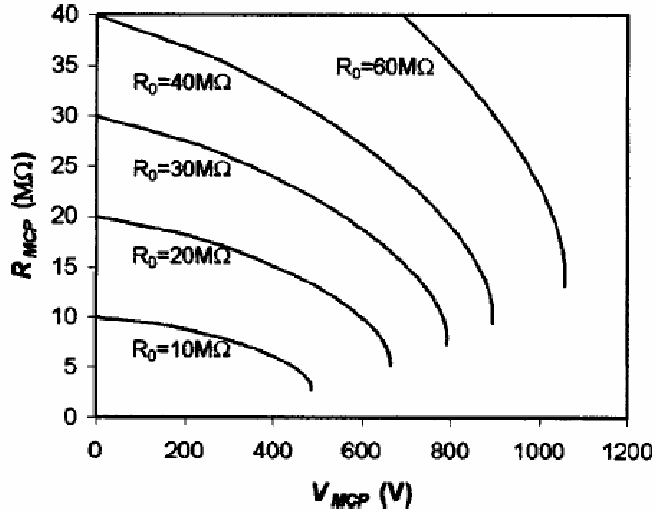

FIG. 6. Calculated resistance of a 40:1 L/D 25 mm diam silica MCP with 6 μm pores (mounted in a chevron stack) as a function of MCP bias V_{MCP} for different values of initial resistance R_0. The initial resistance determines the maximum voltage, which can be applied to the MCP without inducing a thermal runaway.

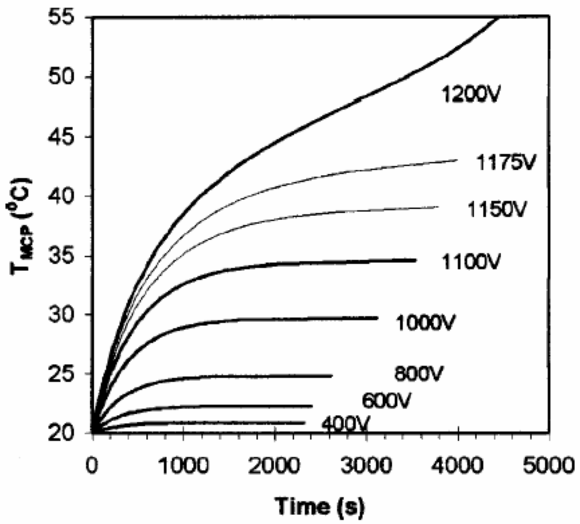

FIG. 7. Calculated temperature of silica MCP as a function of time after V_{MCP} is increased from 0 to a given voltage, indicated on the graph. MCP parameters are as in Fig. 2. For voltages below ~800 V the MCP reaches the thermal equilibrium in a few minutes.

Count rate limitation per illuminated area

Gain drop as a function of event rate for six different sized holes illuminated with 2537Å light. 60mm MCP Z stack.

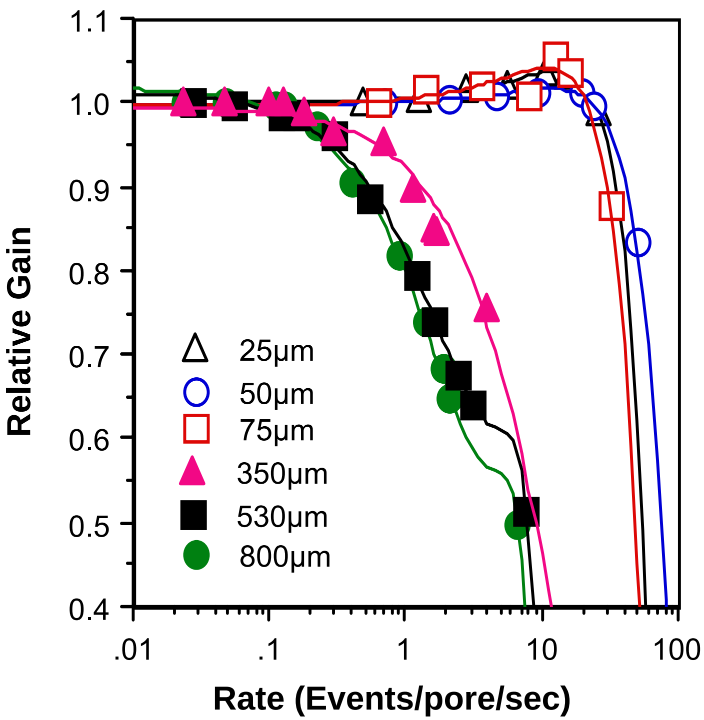

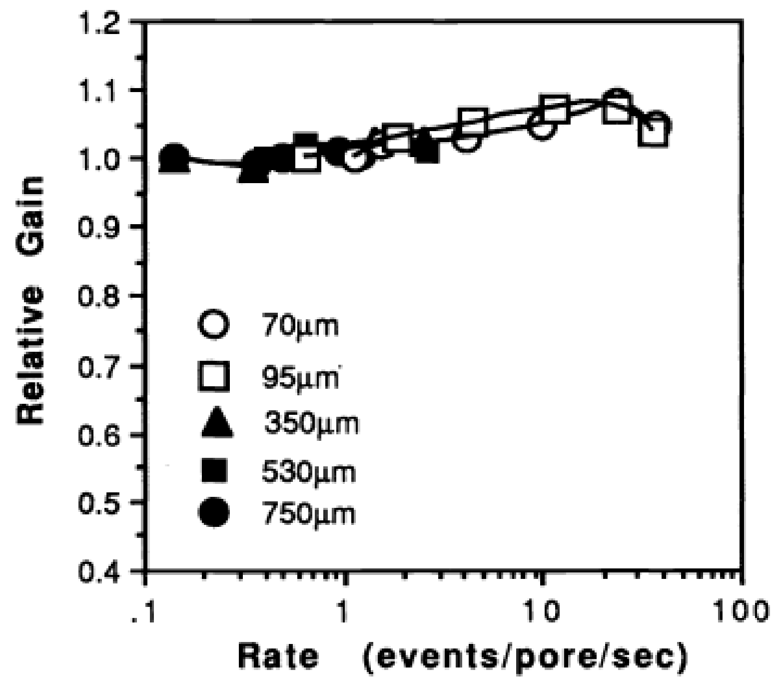

R = 600 MΩ/cm², initial gain ≈1 x 10^7.

R = 120 MΩ/cm², initial gain ≈3 x 10^6.

Count rate limitation is dependent on the area illuminated: larger area can sustain less counts per pore!

O.H.W. Siegmund and Joseph M. Stock, Proc. SPIE 1549, 81 (1991)

MCP gain reduction effect: ageing under irradiation

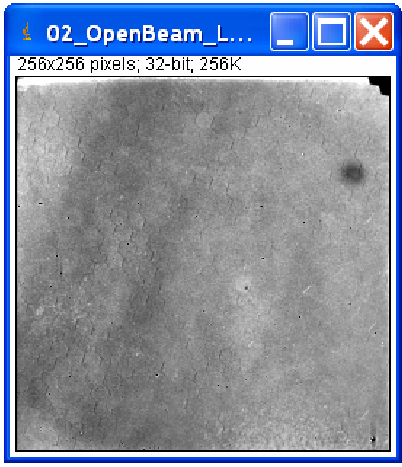

Uniform flat field image

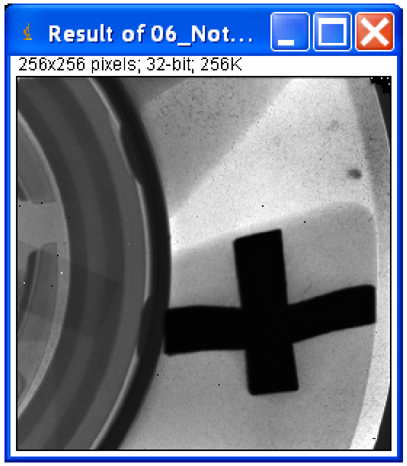

Long integration image
Gain~10^5
Rate >10 MHz/cm^2
Accumulated dose ~0.01 C/cm^2

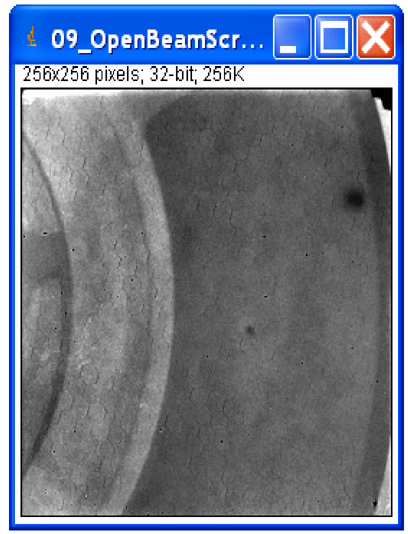

Almost uniform flat field illumination

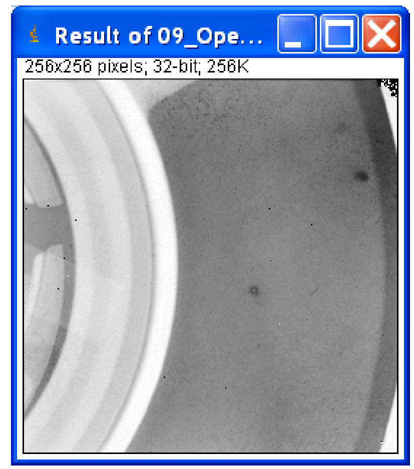

Normalized by initial flat field

No preconditioning of the detector was performed

MCP gain reduction effect: ageing under irradiation

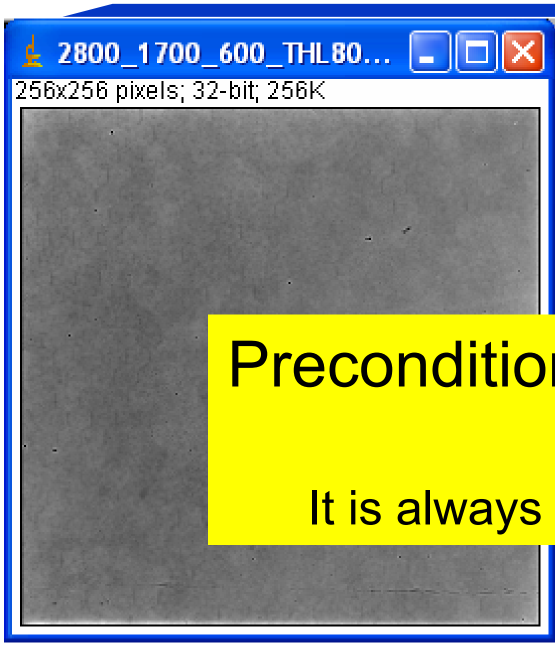

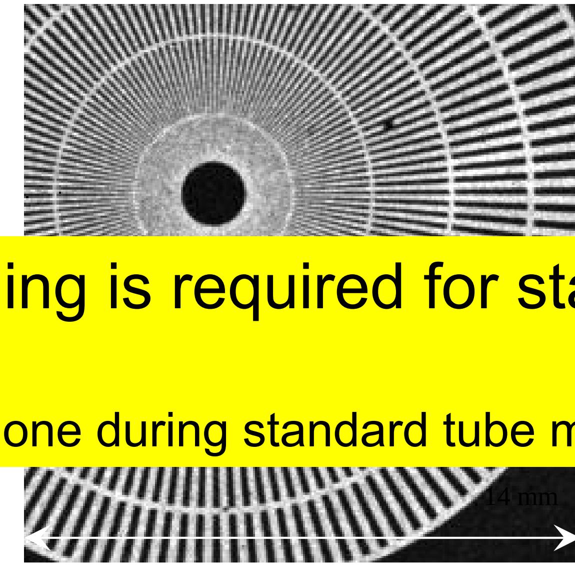

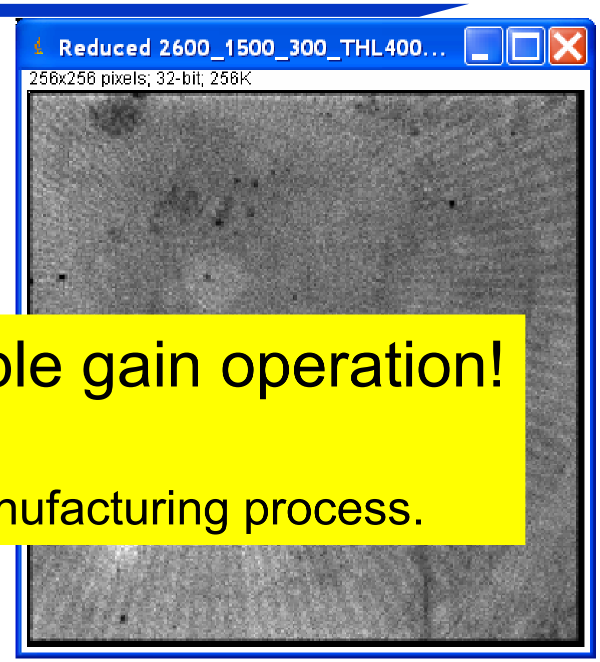

Preconditioning is required for stable gain operation!

It is always done during standard tube manufacturing process.

Uniform flat field image (neutrons)

Resolution mask image
Gain~10^5
Rate ~ 3 MHz/cm^2
Accumulated dose ~0.001 C/cm^2

Almost uniform flat field illuminaiton UV photons

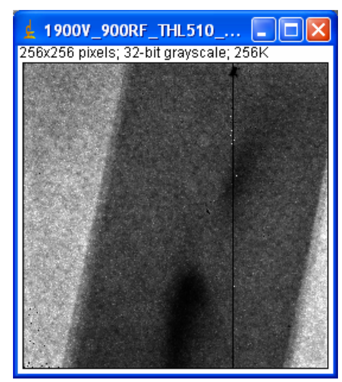

No preconditioning of the detector was performed

Optimization of counting rate

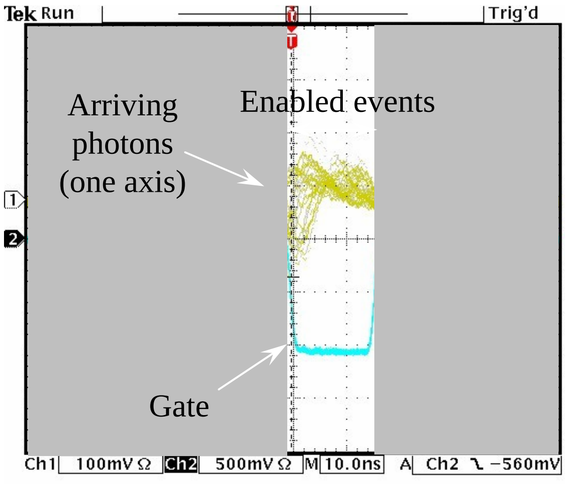

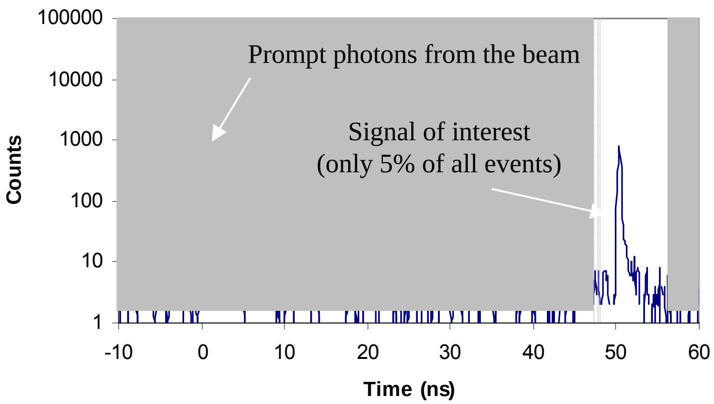

Timing histogram of detected photons.
Secondary peak (~50 ns delayed) seen.

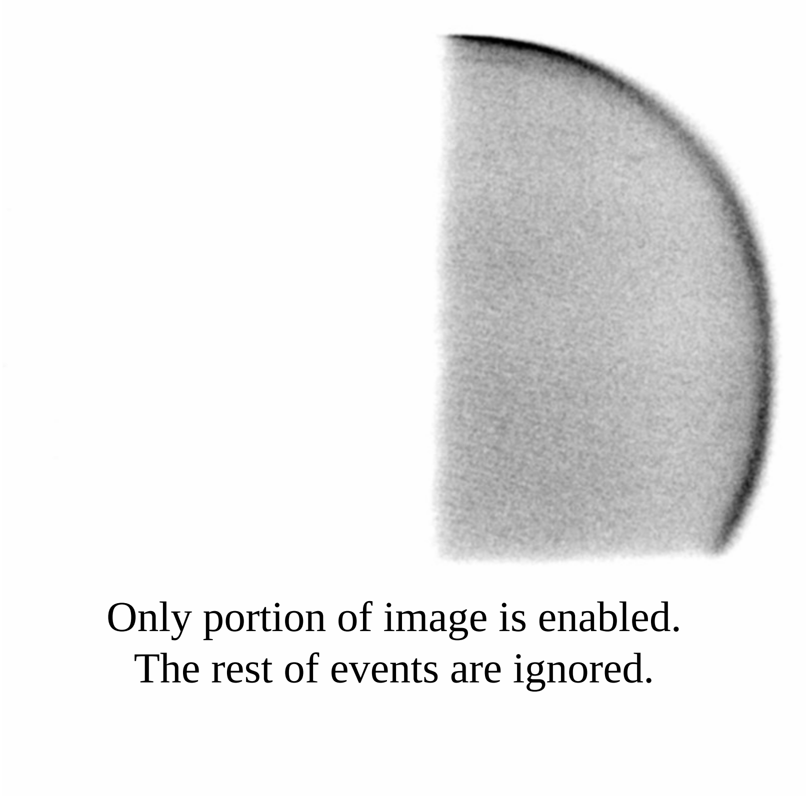

Only portion of image is enabled.
The rest of events are ignored.

A. S. Tremsin, et al., Nucl. Instr. Meth. A 582 (2007) 168.

Bioimaging applications (FRET, FLIM, etc)

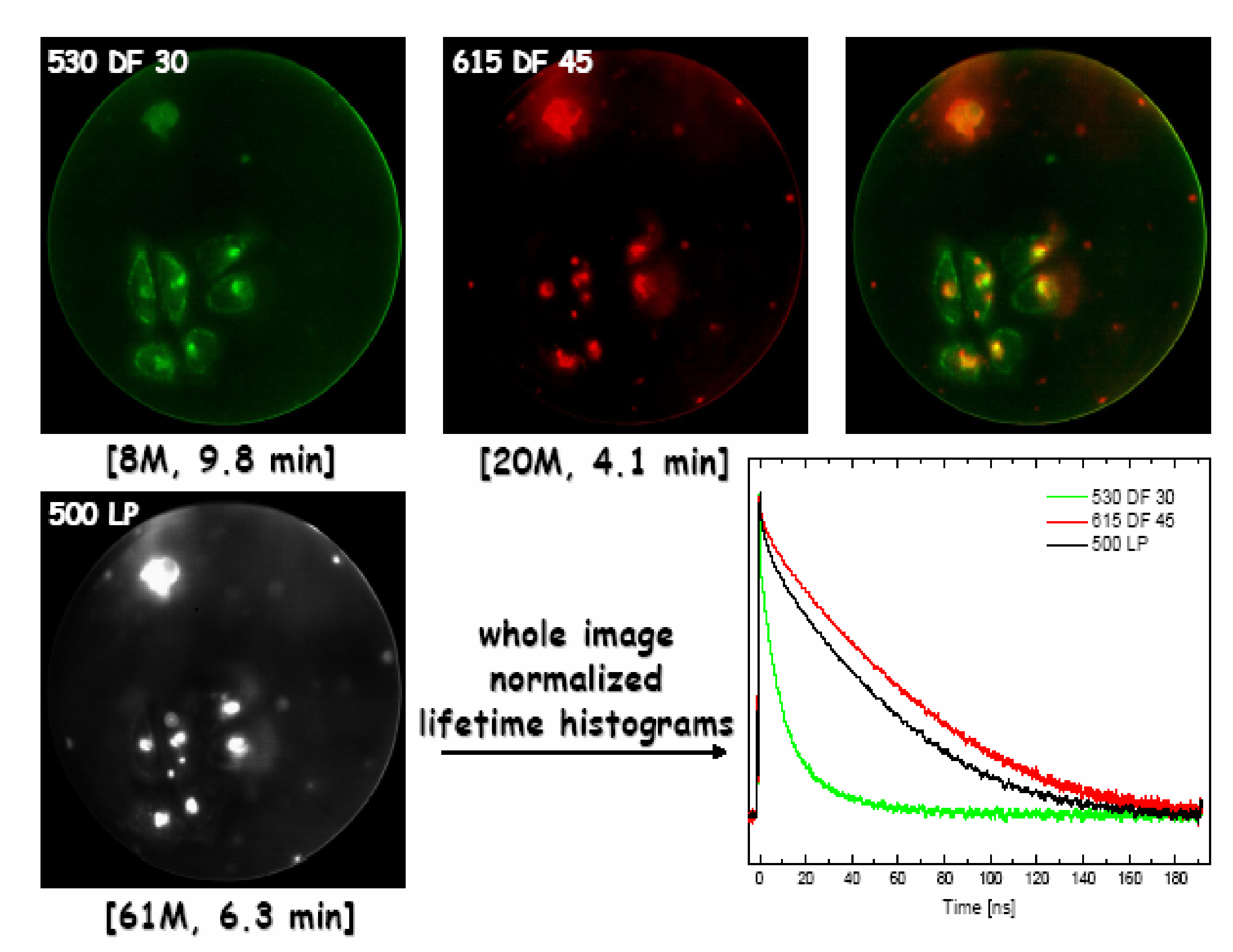

Astrophysics and Earth observing missions

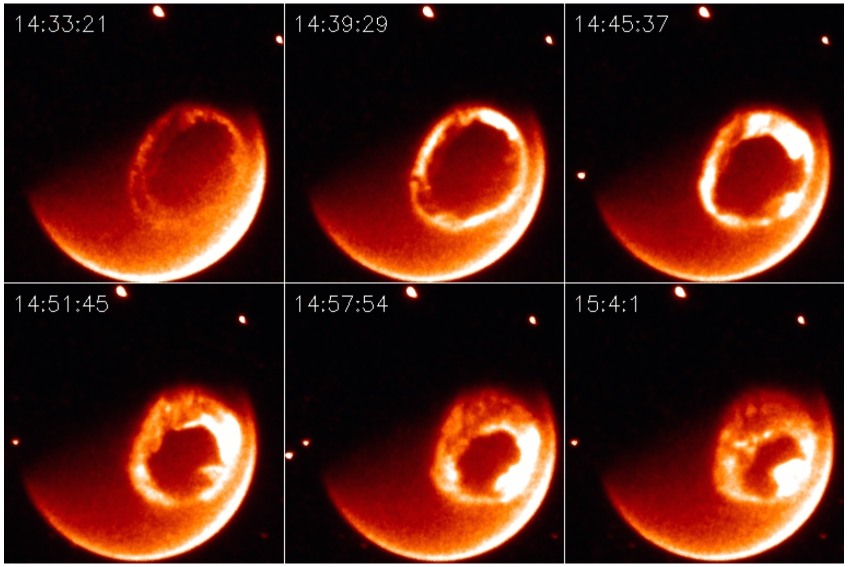

ImageWIC1

Other applications: neutron imaging

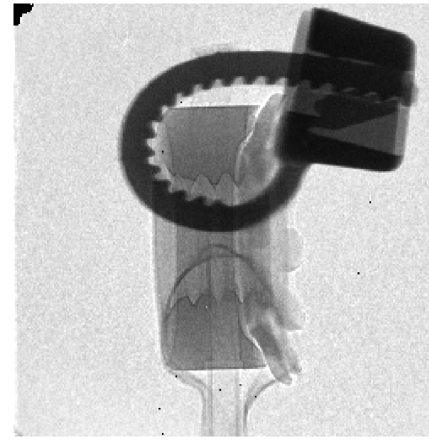

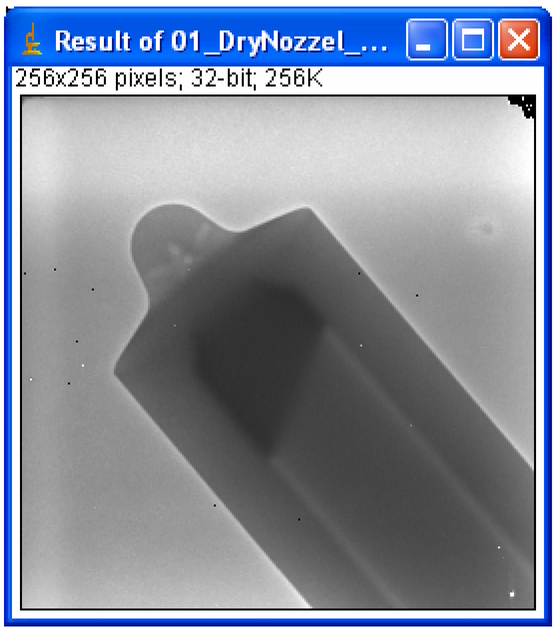

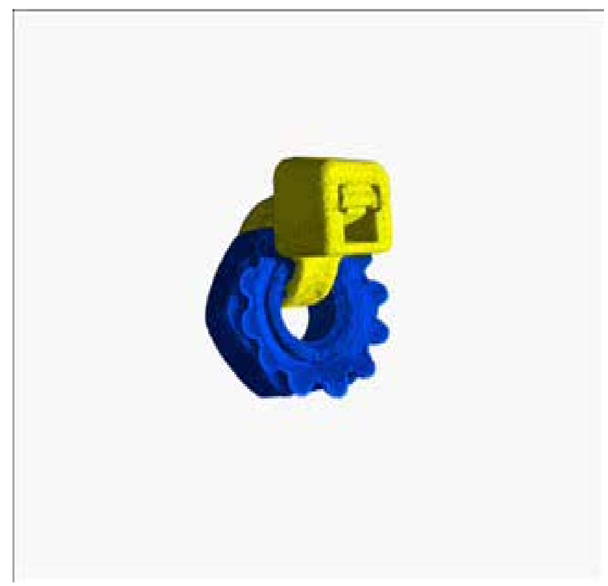

In collaboration with Nova Scientific, Inc. Sturbridge, MA,

Other applications: strain mapping

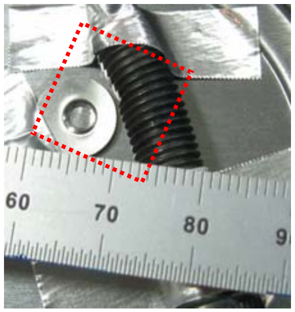

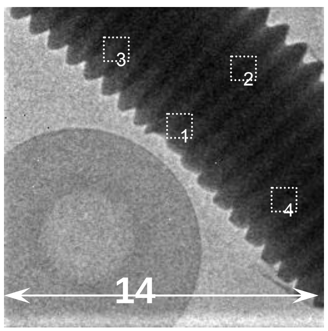

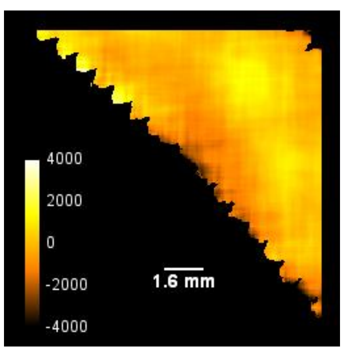

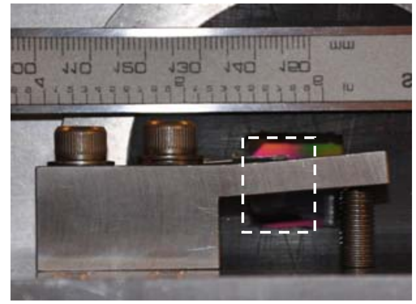

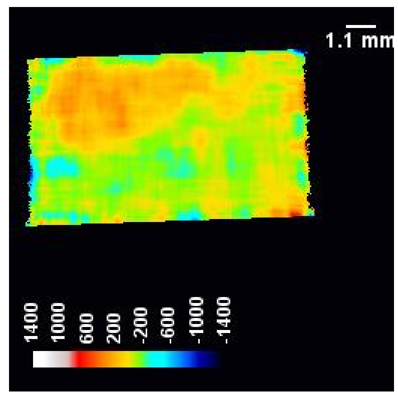

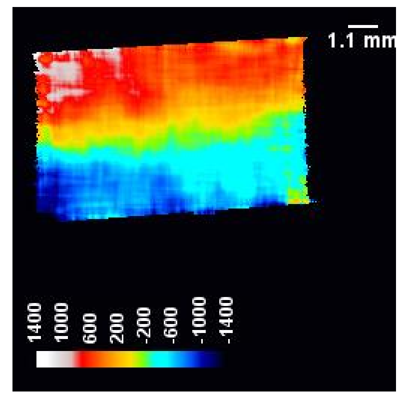

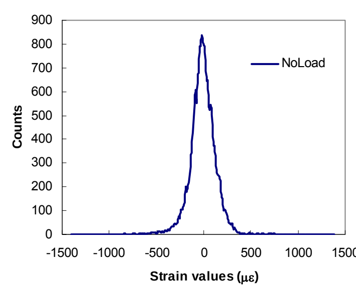

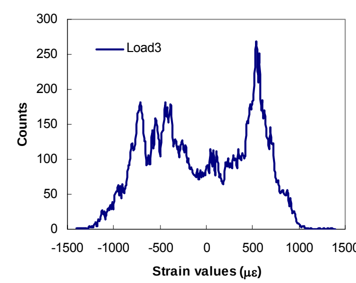

In collaboration with Nova Scientific, Inc. Sturbridge, MA,

Other applications: magnetic field imaging

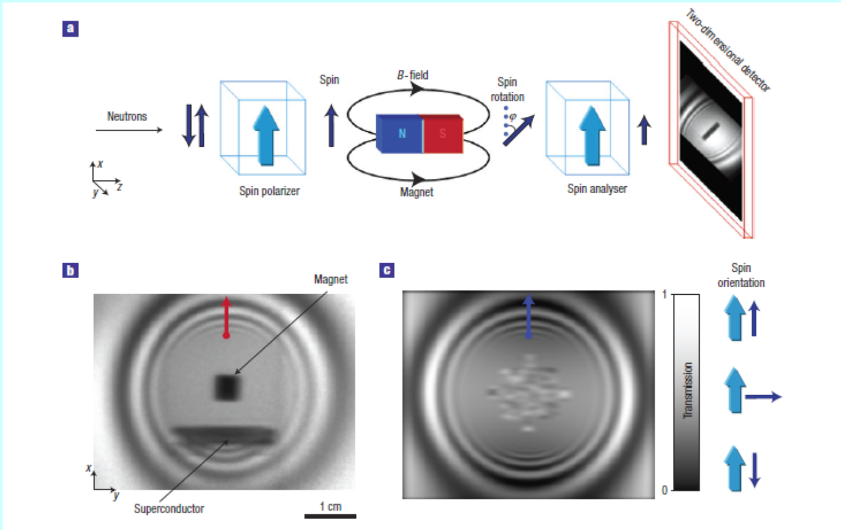

N. Kardjilov et al., Nature Phys. 4 (2008) 399–403

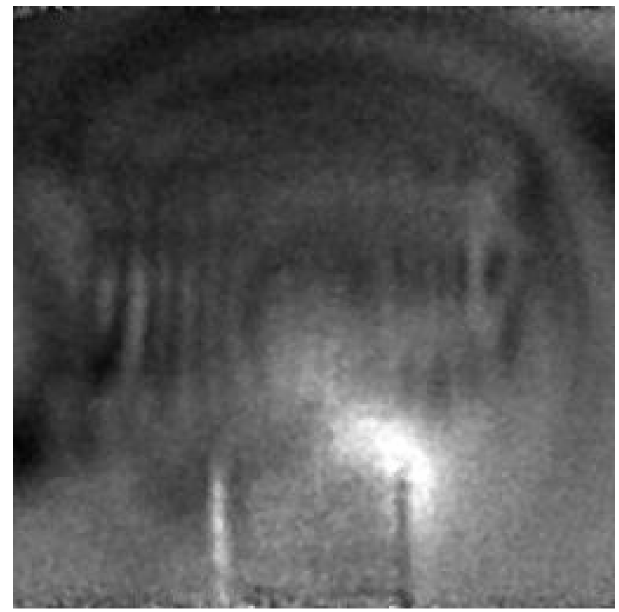

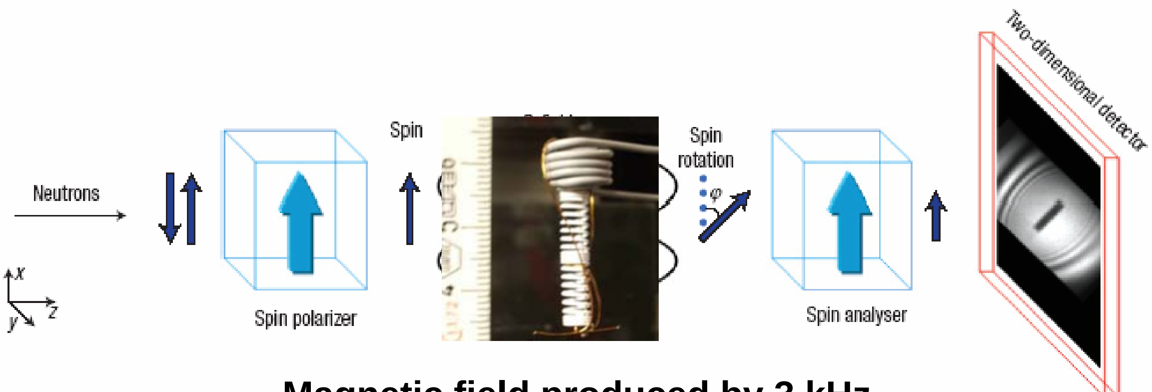

Magnetic field produced by 3 kHz AC current in a coil imaged

In collaboration with Nova Scientific, Inc. Sturbridge, MA,

Possible MCP improvements

- Novel MCP substrates (micromachined)
- Increased lifetime
- Engineered conduction and emission layers
- Controlled saturation and resistance profile (higher dynamic range by offset of saturation to higher input currents)
- Better uniformity / spatial resolution
- Novel photocathode materials / opaque mode / photocathode
- Withstand much higher processing temperature
- Very Low noise

Silicon MCP Geometry

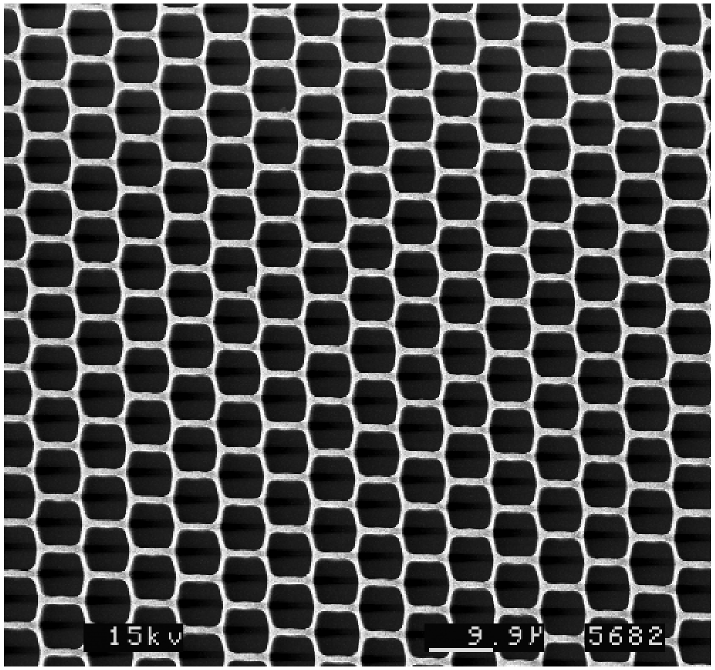

Top view of a hexagonal pore MCP with ~7µm pores showing >75% open area

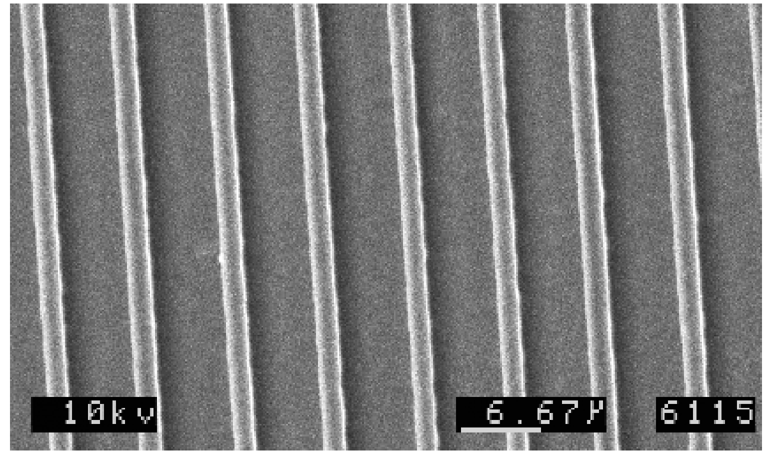

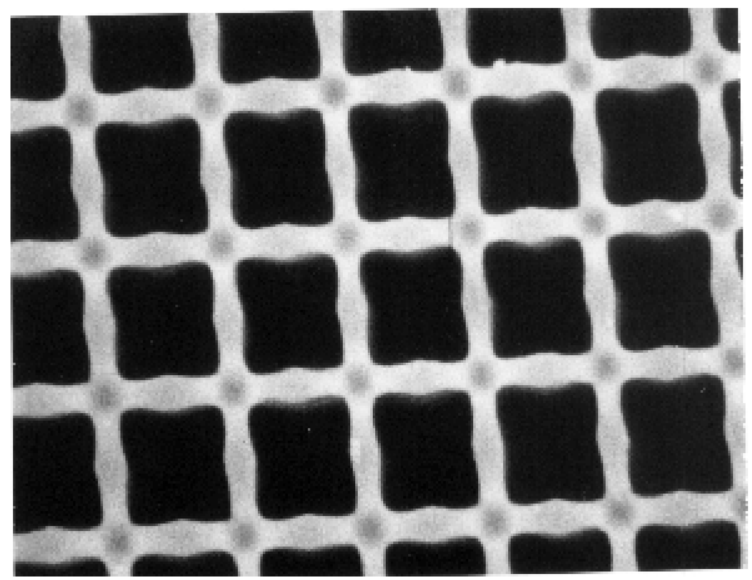

Square pore MCP *2 kx* *6 µm*

Diamond photocathode on Si MCP

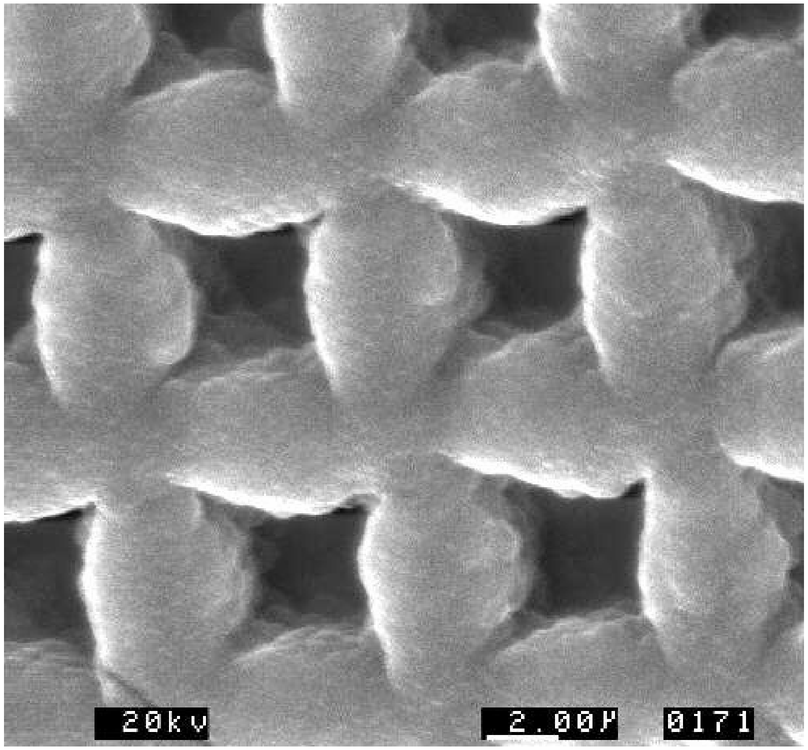

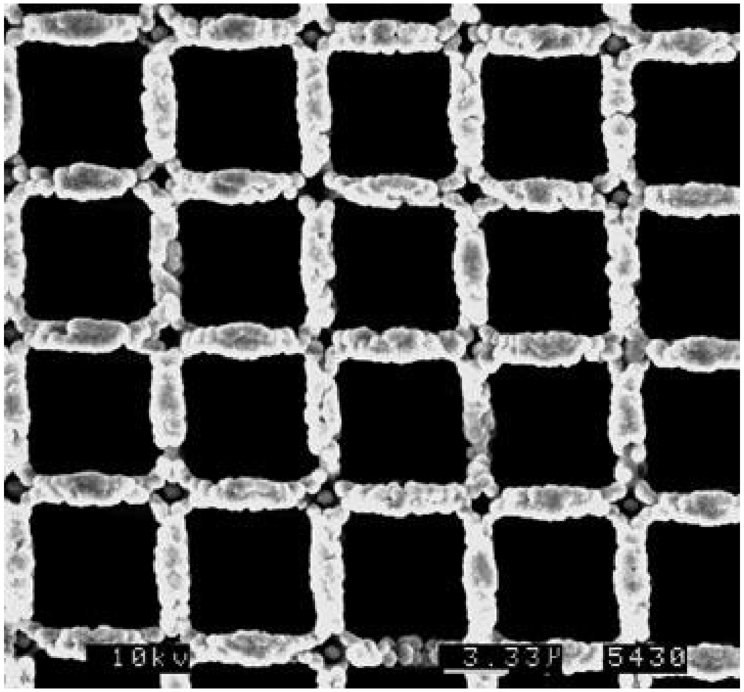

Small grain polycrystalline diamond photocathode

Larger grain diamond photocathode

MCPs with nano-engineered films

Applied over commercial glass MCPs:

50:1 L/D, 4.8 μm pores, ~250 MΩ resistance

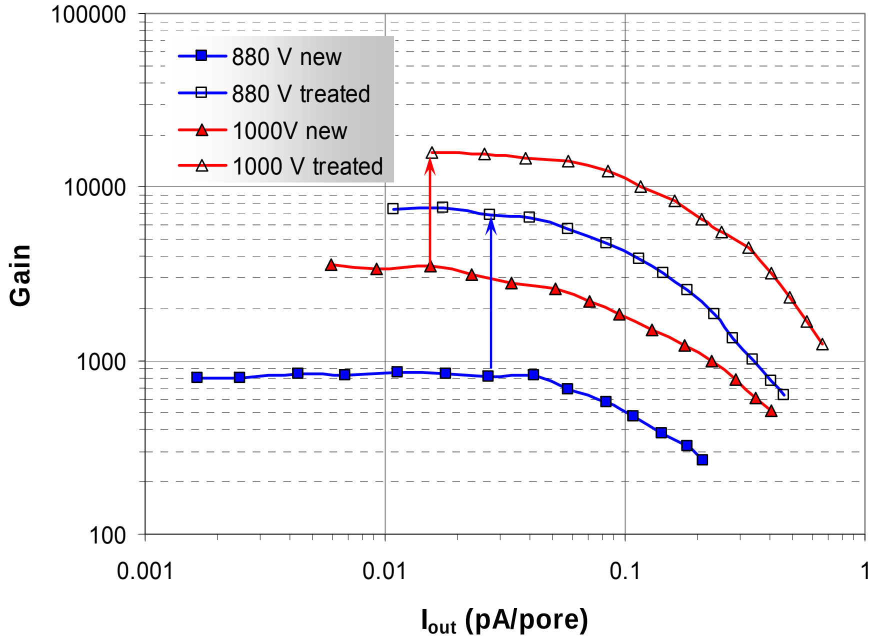

5x-10x gain increase

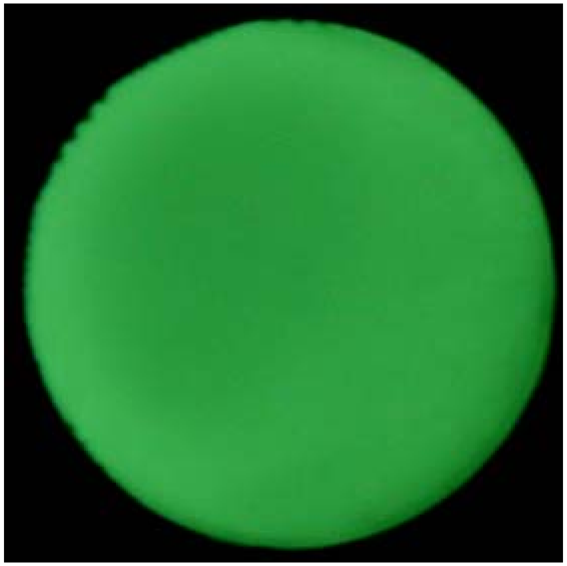

Photograph of the phosphor screen.
Full field illumination image.
MCP is irradiated by a uniform electron flux.

D. R. Beaulieu, et al., Nucl. Instr. Meth. A 607 (2009) 81.

Arradiance, Inc, Sudbury, MA

Nano-engineered conduction and emission films

10 μm pore NO LEAD glass substrate, 40:1 L/D, R~280 MΩ,

gain under electron bombardment

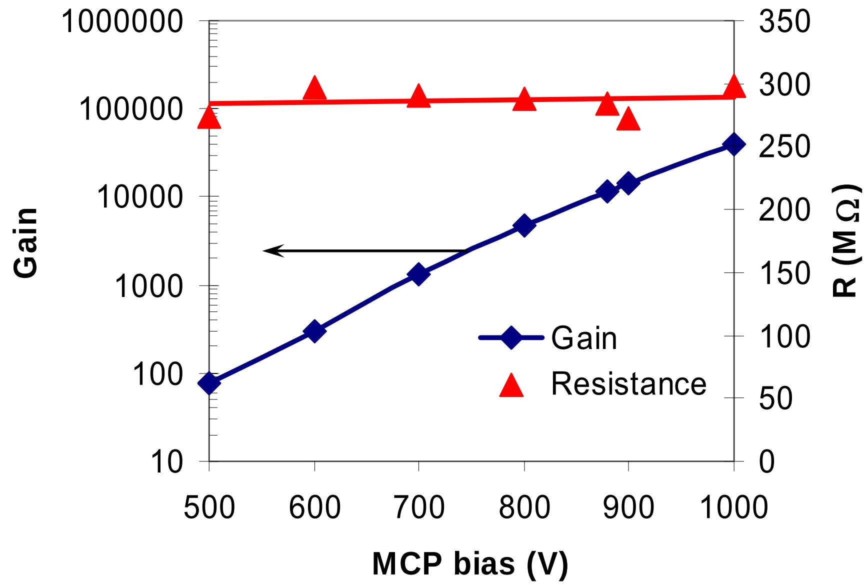

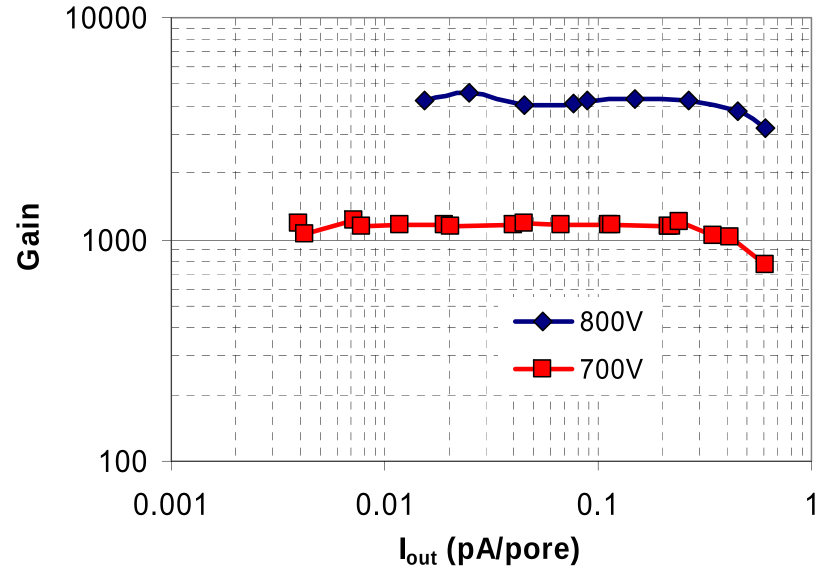

- Stable resistance
- Typical exponential gain increase with bias
- Good gain ~ 40000 at 1000V bias
- Good TCR (comparable to glass MCP values)

D. R. Beaulieu, et al., Nucl. Instr. Meth. A 607 (2009) 81.

Arradiance, Inc, Sudbury, MA

ALD MCP Technology

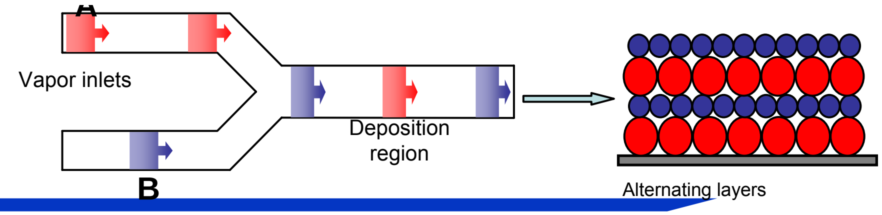

- MCP performance tied to glass composition

ALD:

- Device optimization is de-coupled from substrate.
- Semiconductor processes & process control.
- Materials engineering at the nanoscale
- Functional films composed of abundant,non-toxic materials.
- Advantages:
  - *High conformality (>500:1)*
  - *Scalable to large areas*
  - *Digital thickness control*
  - *Pure films*
  - *Control over film composition*
  - *Low deposition temperatures (50-300°C)*

- Thin film growth that relies on self-limiting surface reactions
- Gas A reacts with a surface
  - *excess precursor & reaction by-product removed.*
- Gas B is introduced to the evacuated chamber – reacts with surface bound A
  - *excess precursor & reaction by-product removed.*
- Repetition of A – B pulse sequence to build film layer-by-layer

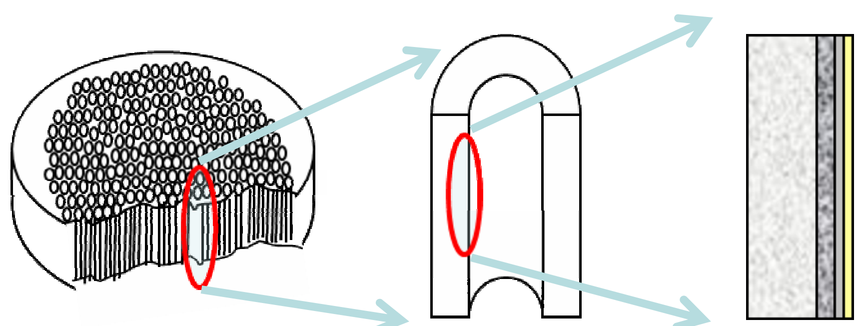

Arradiance, Inc, Sudbury, MA